**IEEE Robotics and Automation Letters (RA-L) paper, presented at ICRA 2026, Vienna, Austria. Cite as RA-L paper.**

# A Novel Robotic Prototype Simulating Oral and Pharyngeal Swallowing with Passive Epiglottis Actuation

Zizhong Zhou[1,2,3], Alberto Gambaruto[1] and Antonia Tzemanaki*[1,2]

***Abstract*—Robotics simulating swallowing hold the potential to enhance our understanding of the swallowing process, support the development of safer texture- or viscosity-modified foods and beverages, and act as medical education tools for both patients with dysphagia and healthcare professionals. Although robotic models in the literature offer insightful actuation mechanisms, many tackle only isolated stages of swallowing, have reduced physiological accuracy, and tend to be mechanically complex and costly. This paper addresses these limitations by developing a novel robotic model that replicates the oral and pharyngeal stages of swallowing, featuring a passive system to simulate the protective closure of the epiglottis. This paper presents the design, function and experimental validation of the robot model. The proposed model can transport thickened fluids from the tongue to the pharynx, preventing aspiration. By enabling passive epiglottis closure, this model advances the physiological fidelity of swallowing robotics, offering insights into actuation mechanisms for future studies.**

***Index Terms*—Biologically-Inspired Robots, Biomimetics, Mechanism Design, Modeling and Simulating Humans, Soft Robot Materials and Design, Tendon/Wire Mechanism.**

## I. INTRODUCTION

SWALLOWING is a complex and precise physiological process in humans. Based on sequence and function, it can be divided into three stages: i) buccal (oral), ii) pharyngeal, and iii) esophageal [1]. This process is controlled by swallowing centers in the brain and a complex peripheral neural network [2], with more than 30 pairs of muscles involved. Disruption of this intricate physiological mechanism can lead to dysphagia. Clinically, dysphagia refers to any condition that affects the safe and smooth passage of food or liquids from the mouth to the stomach [3]. It is classified into oropharyngeal dysphagia (OD) and esophageal dysphagia (ED) [4]. OD refers to difficulty in safely transferring the food bolus from the mouth to the esophagus (i.e., dysfunction of oral and pharyngeal stages of swallowing) [5], while ED refers to impaired bolus transit within the esophageal tube after it has passed through the upper esophageal sphincter (UES) (i.e., dysfunction of esophageal stage of swallowing) [6].

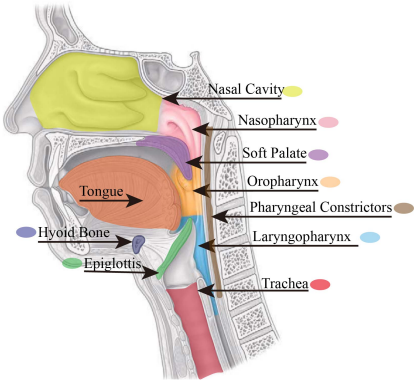


Fig. 1. Upper respiratory and digestive systems (sagittal view), adapted from [7].

Compared to ED, OD more frequently leads to respiratory diseases and serious complications. It is associated with a higher mortality rate, and is more prevalent in certain populations compared with the general population, in which prevalence ranges from 2.3 to 16% [8]: up to 81% among the elderly [4], up to 80% in stroke patients [9], and from 21.9 to 69.5% in patients taking antipsychotic medications [10]. OD can lead to aspiration, causing lung infections or choking, which may consequently increase mortality in elderly and frail individuals [5]. Currently, one of the most commonly used non-invasive management strategies of dysphagia, and especially OD, is swallowing therapy, which involves dietary modifications that change the texture and viscosity of food or liquid intended both to enhance swallowing safety [11]–[13] and to facilitate swallowing exercises (e.g., oral sensory–motor therapy [14]). Over the past decades, efforts have been made to study the modification of food texture and liquid viscosity [15]–[17]. However, texture-modified foods (TMF) and viscosity-modified beverages (VMB) still suffer from poor palatability, resulting in low compliance rates [12], [18]. Additionally, a white paper by the European Society for Swallowing Disorders (ESSD) emphasizes that enhancements are needed to mitigate high-viscosity residues, improve taste, and increase acceptance among patients with OD [12], [19]. Consequently, efforts to refine dietary modifications for dysphagia management are still ongoing. However, conducting in-vivo swallowing experiments on patients when addressing this matter is neither safe nor ethical. Developing robotic swallowing simulators can

Manuscript received: July, 7, 2025; Revised December, 9, 2025; Accepted December, 16, 2025.

This paper was recommended for publication by Editor Jessica Burgner-Kahrs upon evaluation of the Associate Editor and Reviewers' comments.

[1]All authors are with the School of Engineering Mathematics and Technology, University of Bristol, Bristol BS8 1TH, UK Antonia.Tzemanaki,alberto.gambaruto}@bristol.ac.uk

[2]Zizhong Zhou and Antonia Tzemanaki are also with the Bristol Robotics Laboratory, UK

[3]Zizhong Zhou is also with Zhejiang University, China skewink@163.com

Digital Object Identifier (DOI): see top of this page.

**IEEE Robotics and Automation Letters (RA-L) paper, presented at ICRA 2026, Vienna, Austria. Cite as RA-L paper.**

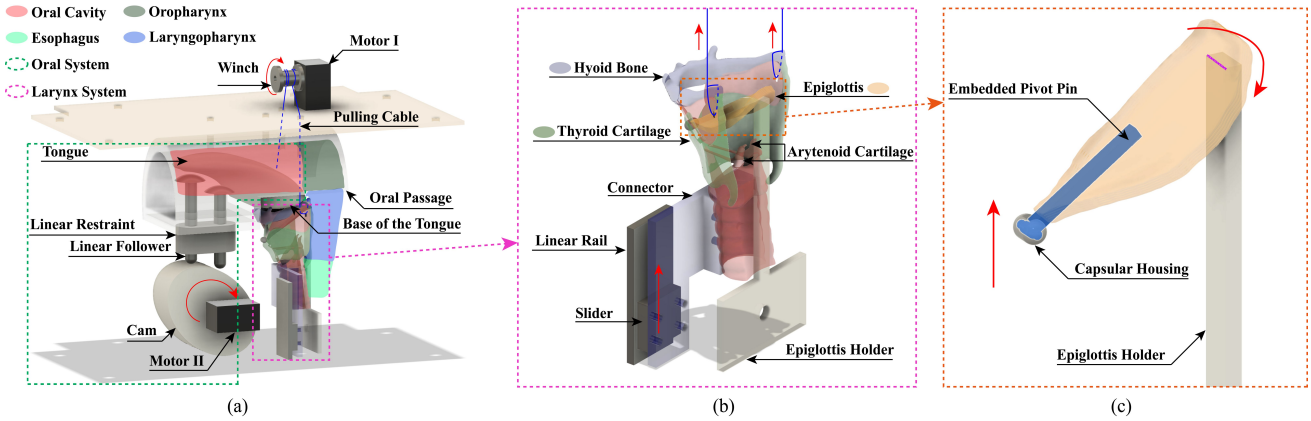


Fig. 2. Design of the proposed swallowing robot. (a) Overview of the model. (b) The larynx system. (c) The epiglottis.

provide a safer and more feasible alternative to test specialized food materials [20].

In recent years, research on robots that simulate oral and pharyngeal stages of swallowing has begun to emerge [21]–[26]. These robots either do not incorporate epiglottis actuation, assuming that it remains closed (normal swallowing) [25] or open (extremely pathological swallowing) [21], [22], or actively control its movement [23], [24], [26]. In [23], the simulation of epiglottic motion was actively achieved by a motor-driven "epiglottic metal stem" embedded within a silicone-fabricated anatomical epiglottis structure. In [24], the simulated epiglottis was designed as a tendon-driven flexible hinge structure, where tension applied to the tendon via a motor-operated pulley caused the epiglottis to tilt and cover the airway. By contrast, [26] implemented the epiglottis as a rigid flag-pole-like structure, where a motor actively rotated the pole axially to pivot the flag-like epiglottis and cover the trachea. However, as an essential step in safe swallowing [27], the protective closure of the epiglottis is commonly recognized as a primary consequence of the hyoid and laryngeal elevation, rather than being actively actuated by a specific epiglottis muscle or controller [28]. Replicating this mechanism in a passive way aligns with established physiological and anatomical evidence [28], [29], and thus increases the likelihood of clinical translation and application [30], [31]. However, as multiple complex factors are involved in this process [32], it is difficult to simulate this movement passively.

In this paper, we present a robotic anatomical model that emulates the oral and pharyngeal stages of human swallowing. Instead of introducing a dedicated actuator, the proposed model implements a passive epiglottis actuation mechanism that simulates the protective closure of the epiglottis to prevent aspiration. By addressing prior limitations related to the physiological fidelity of epiglottis movement, this study serves as an initial framework and inspiration for future research into swallowing robotics, and, thereby, enhances its prospects for applications in food research and the healthcare industry.

The remainder of the paper is structured as follows: Section II presents the design, simulation, and implementation of the robotic swallowing model, as well as the anatomical and physiological principles of swallowing that motivate our design. Section III presents the characterisation of the motion of the model and the experimental evaluation of swallowing. Section IV concludes and discusses future work.

## II. Materials and Methods

### A. Physiology of Oral and Pharyngeal Swallowing

This section briefly describes the steps of the swallowing process and identifies the important structures involved in the proposed prototype. The features of the pharynx are shown in Fig. 1. The oral stage is the initial stage of swallowing. After the preparation of the food bolus, the constriction of the muscle groups of the tongue [33] causes the tip of the tongue to curl, and the middle and rear sections to rise in a peristaltic sequence. This action presses the bolus against the palate and propels it to the oropharynx.

As the bolus enters the oropharynx, the soft palate rises to seal the nasal cavity, preventing aspiration [33]. Upon reaching the junction of the tongue, soft palate, and pharyngeal constrictor wall, it stimulates the mucosal receptors in the pharynx and thus, triggers the pharyngeal stage of swallowing. Subsequently, the hyoid bone and the larynx elevate. As the epiglottis leaf is deeply embedded in the larynx, its position remains relatively unchanged during this elevation. However, this elevation drives the epiglottis stem to rise. Consequently, the orientation of the epiglottis switches from near-vertical to horizontal and tilts downward passively. This movement closes the laryngeal vestibule and covers the trachea, preventing the bolus from entering the lungs [32], [34]. Meanwhile, the pharyngeal constrictors constrict in a sequence to generate a peristaltic wave, pushing the bolus down to the UES [1].

### B. Mechanical Design and Actuation Mechanism

The proposed model (Fig. 2) focuses on replicating the peristaltic elevation of the tongue and the elevation of the larynx, in order to investigate the swallowing motions generated by these movements and evaluate the overall swallowing safety of the model. It comprises two systems, the oral and the laryngeal, connected by bonding the base of the tongue to the hyoid bone with adhesive (Fig. 2(b)). In the oral system, a silicone model of the tongue is placed within the oral passage that represents the oral cavity and the oropharynx. Driven by a motor (motor II in Fig. 2(a)), the cam mechanism rotates and

**IEEE Robotics and Automation Letters (RA-L) paper, presented at ICRA 2026, Vienna, Austria. Cite as RA-L paper.**

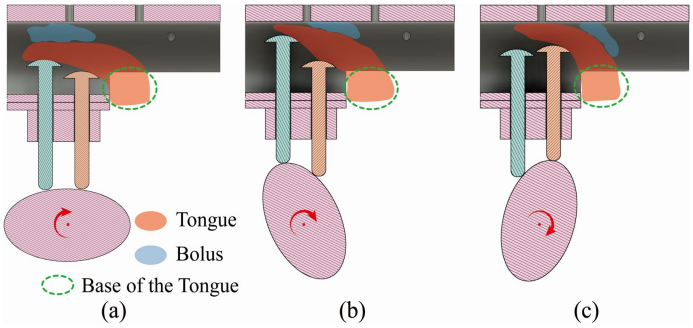


Fig. 3. Actuation of the tongue: (a) the swallowing has not started, (b) the cam rotates and drives the anterior follower to push the tip of the tongue against the palate, and (c) the cam rotates and drives the posterior follower to push the midsection of the tongue against the palate.

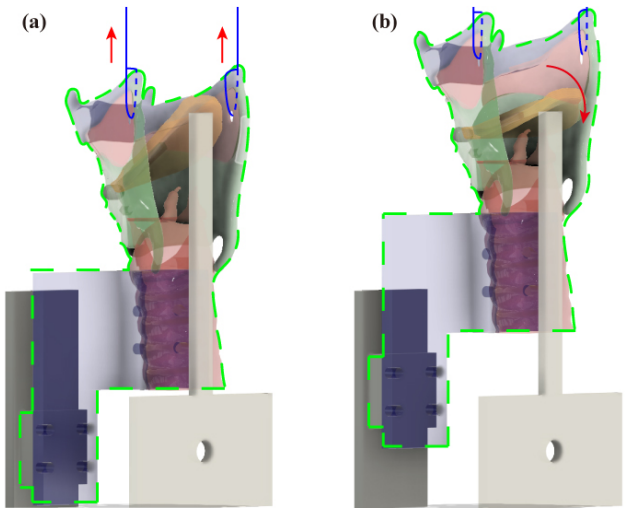


Fig. 4. Actuation of the larynx and the epiglottis. (a) State 1. (b) State 2.

drives the follower vertically. This motion sequentially pushes the tip and midsection of the tongue against the palate and propels the food bolus toward the base of the tongue (Fig. 3). In the laryngeal system (Fig. 2(b)), the polylactic acid (PLA) larynx is connected to a linear rail fixed to the acrylic frame. In the larynx, a 'capsule' houses the cylindrical tip of the pivot pin (Fig. 2(c)), with the rest of the part embedded in the epiglottis. The capsular housing is bonded to the thyroid cartilage with adhesive. All parts were designed in Fusion360 using the dataset by [35], [36].

As the bolus reaches the base of the tongue, a motor (motor I in Fig. 2(a)) rotates the winch, pulling the cable, and lifting the larynx vertically (Fig. 4(a), State 1). This motion elevates the base of the tongue and presses it against the palate, pushing the bolus into the oropharynx. Meanwhile, as the distal end of the epiglottis is fixed to the epiglottis holder, the elevation of the larynx causes an upward movement of the capsule and generates a force that acts on the embedded pivot pin. This force creates a torque that causes the epiglottis to undergo a passive downward tilting motion (Fig. 4(b), State 2). As this model focuses on the efficacy of passive epiglottis tilting in preventing aspiration, the pharyngeal constrictor muscles were not modeled, and upon reaching the oropharyngeal cavity, the bolus descends through the pharynx under gravity.

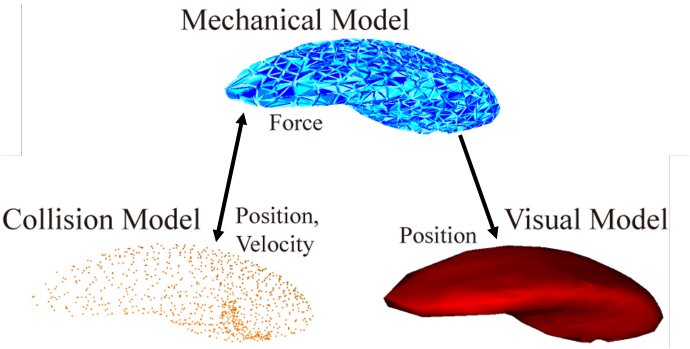


Fig. 5. The three models of the simulated tongue in SOFA.

### C. Modeling and Simulation

*1) Simulation Environment and Configuration:* To better explore and replicate the coordinated and sequenced dynamics of swallowing in a robotic system, a physics-based computational model was established to simulate the interaction and actuation of the designed components using SOFA (Simulation Open Framework Architecture) [37].

In this environment, the simulated objects are represented by three models. As shown in Fig. 5, the tongue consists of a mechanical model, a collision model, and a visual model (surface), used to simulate the internal mechanical behavior (deformation in this case), collisions, and visualization, respectively. These models are loaded from the 3D meshes of the CAD files which are generated from Autodesk Fusion. In Fig. 5, the mappings (black arrows) propagate positions and velocities from the mechanical model to the collision model. As the collision model receives force from other collision models (linear followers in this case), that force is mapped to the mechanical model to induce deformation and movement. Subsequently, the mechanical model maps the deformed positions to the visual model for display. Finite element modeling with tetrahedral elements is employed to compute the deformation of the models.

To better observe the interactions between the different swallowing components of the system, the actuation structure in the simulation was simplified. The linear followers and the larynx were programmed to elevate sequentially with preset speeds and distances. The tongue and the epiglottis were directly attached to the larynx through the *BilateralLagrangianConstraint* law [38]. This SOFA component enforces a holonomic equality constraint

$$\Phi(x_1, x_2) = 0 \tag{1}$$

between two Lagrangian mechanical objects, ensuring that a pair of selected vertices $(x_1, x_2)$ on each object maintain a fixed relative position. The distal end of the epiglottis is directly fixed with the *FixedProjectiveConstraint* law [39]. This enforces that the degrees of freedom (DOFs) of selected points on the epiglottis remain at their initial velocity (zero in this case) by projecting the linear response of the system onto a subspace that excludes those DOFs. The specific simulation parameters are shown in Table I.

*2) Simulation Results:* At 0.00s (Fig. 6(a)), the anterior linear follower begins its upward movement. At 0.43s (Fig. 6(b)),

**IEEE Robotics and Automation Letters (RA-L) paper, presented at ICRA 2026, Vienna, Austria. Cite as RA-L paper.**

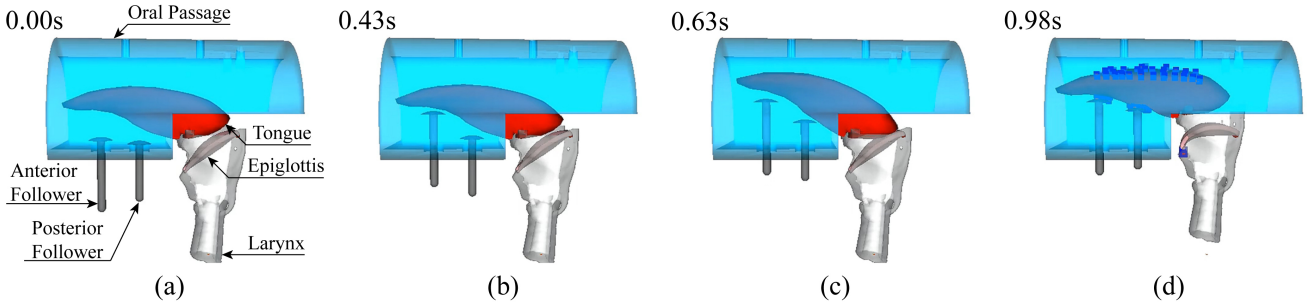


Fig. 6. Simulation of the model operation in SOFA. (a) The anterior linear follower starts to move. (b) The posterior linear follower starts to move. (c) The larynx starts to elevate. (d) Completion of operation (blue dots represent contact detection).

TABLE I
SIMULATION CONFIGURATION

| Parameter | Value |
|---|---|
| Young's modulus of tongue | 111.6 kPa [40] |
| Poisson's ratio of tongue | 0.49 [41] |
| Young's modulus of epiglottis | 290 kPa [42] |
| Poisson's ratio of epiglottis | 0.25 [42] |
| Time step | 0.01 s |
| Contact distance | 2 mm |
| Alarm distance | 3 mm |

the anterior follower initiates tongue elevation, and the upward movement of the posterior follower is activated. From 0.63s (Fig. 6(c)), the larynx elevates, pushing the base of the tongue upward. By 0.98s (Fig. 6(d)), the process is complete, with the epiglottis tilting downward covering the trachea. Moreover, as illustrated in Fig. 6(d), contact is detected between the tongue and the palate, indicating that the elevation of the tongue and larynx is sufficient to propel food from the oral cavity into the pharynx.

### D. Fabrication and Implementation

With the general structure and operation mechanism proven feasible in simulation, the prototype shown in Fig. 7 was manufactured. The entire system is mounted on a 290 × 200 × 200 mm aluminum frame, with acrylic boards connecting the motors, actuators, anatomical structures, and frame. Power is supplied to the motors by a 9V lithium battery through an L298N motor driver. The control of the system is implemented by an OpenRB-150 microcontroller.

To replicate swallowing structures for anatomical fidelity, the tongue and the epiglottis were fabricated from silicone. The CAD models of the tongue and the epiglottis were hollowed out, and 3D printed for silicone moulding. The longer part of the 3D-printed pivot pin (PLA) (Fig. 2(c)) was inserted into the epiglottis mould before the silicone cured. Its cylindrical tip was placed in the capsular housing on the thyroid cartilage to enable rotation. Among commonly used silicone materials, Ecoflex 00-30, with Young's modulus of 0.1 MPa [43], comparable to that of active tongue [40], was chosen for tongue fabrication. The epiglottis was moulded using Dragon Skin 10NV, with Young's modulus ranging from 0 to 0.3 MPa [44]. Two additional pieces, made from Dragon Skin 10NV, were shaped into quadrangular membranes to bond

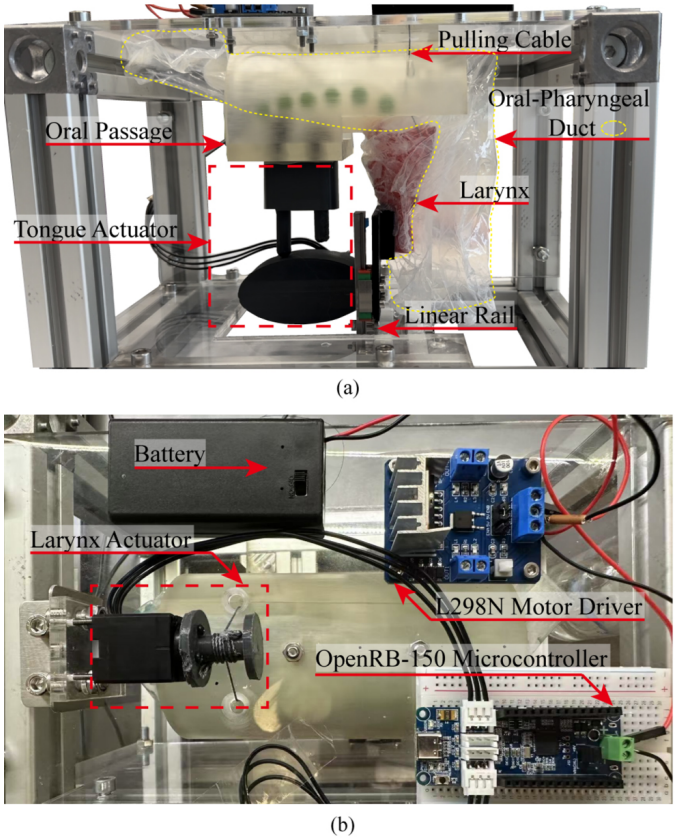


Fig. 7. Overview of the proposed swallowing robot. (a) Front view. (b) Top view.

the arytenoid cartilage (shown in Fig. 2(b)) to the sides of the epiglottis (Fig. 9(a)).

To ensure effective propulsion of food into the pharynx and simplify movement, the oral passage was fabricated from rigid, semi-transparent resin (Formlabs Clear Resin V4), to prevent passive deformation and allow observation of internal movements. For continuous food passage, the oral and pharyngeal ducts were fabricated as a single piece (shown in Fig. 7(a)) from polyethylene (PE). The upper part of it serves as the oral cavity, and the lower part serves as the pharynx. The larynx was also 3D printed with PLA, removing the epiglottis for separate fabrication from silicone.

The actuation system is based on the mechanism described in Section II-B. Notably, in the tongue mechanism, the rota-

**IEEE Robotics and Automation Letters (RA-L) paper, presented at ICRA 2026, Vienna, Austria. Cite as RA-L paper.**

tional speed of the cam and the linear follower length can be adjusted to simulate abnormal swallowing for future studies. Similarly, in the larynx, the winch angle of rotation can also be adjusted to simulate abnormal laryngeal elevation during swallowing.

## III. Experiments and Results

The experimental evaluation includes two key aspects: recording and analyzing the motion of the tongue and epiglottis, as well as conducting food swallowing experiments to assess swallowing safety.

### *A. Motion of the Tongue and the Epiglottis (Without food)*

*1) Experiment Setup:* Six green markers were placed on the side of the tongue (Fig. 8), and five green markers were placed on the posterior edge of the epiglottis (Fig. 9). The motion of the tongue and the epiglottis were recorded and analyzed by tracking the green markers. The videos were first processed in the HSL (Hue, Saturation, Lightness) color model to accentuate green hues. Then, each frame was converted to the HSV (Hue, Saturation, Value) color space. A binary mask was then generated by thresholding pixels within the specified green range (H: 35–85, S: 100–255, V: 100–255). This mask was refined with erosion and dilation to suppress noise and fill small gaps. Finally, contours of sufficiently large green regions were detected, and their centroids were marked red for better observation.

*2) Results:* Fig. 8 compares the motion of the artificial tongue of the prototype to a human tongue from a Magnetic Resonance Imaging (MRI) scan of swallowing [45]. In the MRI, the surfaces of the tongue are marked green. The positions of the larynx are represented by those of the hyoid bone (circled in yellow). As illustrated in Fig. 8(a)-(d), the motion pattern of the artificial tongue broadly aligns with that observed in MRI of real human swallowing, both exhibiting a sequential peristaltic motion from anterior to posterior. The artificial and human tongues reach comparable key poses at a similar rate. The laryngeal movements in the MRI, occur only between Fig. 8(c) and Fig. 8(d), which corresponds to the behavior of the model.

Fig. 9 illustrates the motion of the artificial larynx and epiglottis of the model during swallowing. The absolute position of the epiglottis tip remains constant; however, as the larynx elevates, the epiglottis tilts downward passively, reducing its distance from the tracheal opening, and gradually covering the airway to prevent food aspiration.

Fig. 10(a) and (b) show the position of the markers on the tongue and the epiglottis, respectively, with respect to time. From Fig. 10(a), it can be observed that markers 1, 2, and 6 lie slightly below markers 3–5, indicating that the tongue tip and root are positioned lower than the midsection, consistent with the MRI image in Fig. 8(a). At this stage, markers 1–3 are sequentially lower than the subsequent markers. After rotation, the vertical order of these three markers reverses, demonstrating that they elevate in sequence as the cam turns, producing a peristaltic motion that propels the food bolus inward, which aligns with the physiology of the oral stage of swallowing. Fig. 10(b) shows that the epiglottis markers exhibit no significant vertical displacement, only minor oscillations within 1 mm. This indicates that the system replicates the passive tilting of the epiglottis, achieving its protective closure via laryngeal elevation rather than active epiglottis control.

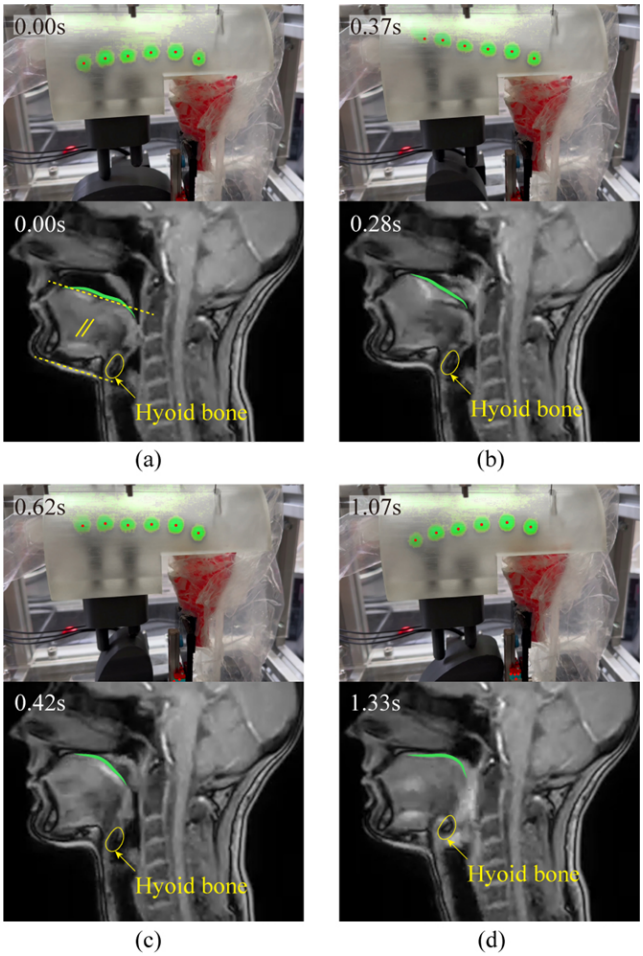


Fig. 8. Comparison of artificial and real tongue during swallowing. (a) the dorsal surface of the tongue exhibits a slight inverted-U profile, with its mid-section elevated above both the tip and the root. In the MRI, this appears as the mid-section lying above a plane parallel to the mandibular plane at the tongue surface, while the tip and root lie below that plane. (b) the tip of the tongue in both the prototype the MRI are elevated. (c) the midsections of the tongue in both the prototype and the MRI are elevated. (d) the larynx rises in both images, elevating the tongue root against the palate.

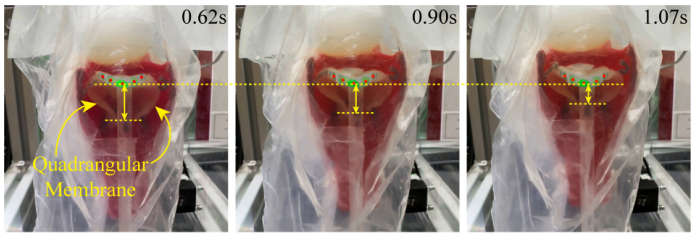


Fig. 9. Upward Motion of the artificial larynx and protective closure of the epiglottis. From (a) to (c), as the larynx elevates, the epiglottis tilts downwards to cover the trachea.

**IEEE Robotics and Automation Letters (RA-L) paper, presented at ICRA 2026, Vienna, Austria. Cite as RA-L paper.**

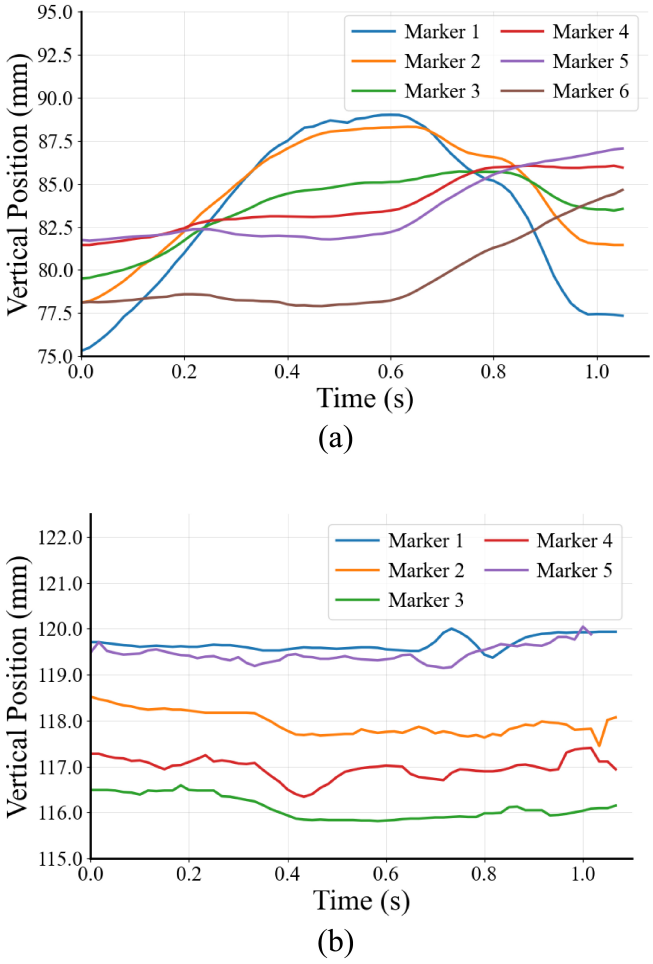


Fig. 10. Kinematic patterns of the tongue and the epiglottis. (a) Vertical displacements of tongue markers over time. Markers 1–6 represent the six markers on the tongue, numbered sequentially from the tip to the root. (b) Vertical displacements of epiglottis markers over time. Markers 1–5 represent the five markers on the epiglottis, numbered sequentially from left to right.

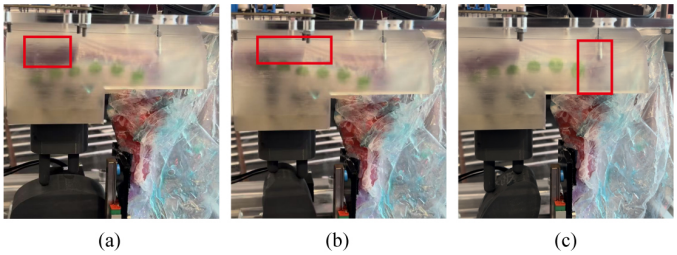


Fig. 11. Swallowing experiment. (a) Before swallowing begins, the majority of the fluid accumulates at the opening of the oral-pharyngeal duct. (b) As the tip of the tongue reaches the palate, part of the fluid is propelled inward. (c) When the cam completes its rotation and the larynx reaches its maximum position, most of the fluid enters the oropharynx. It then descends through the pharynx under gravity.

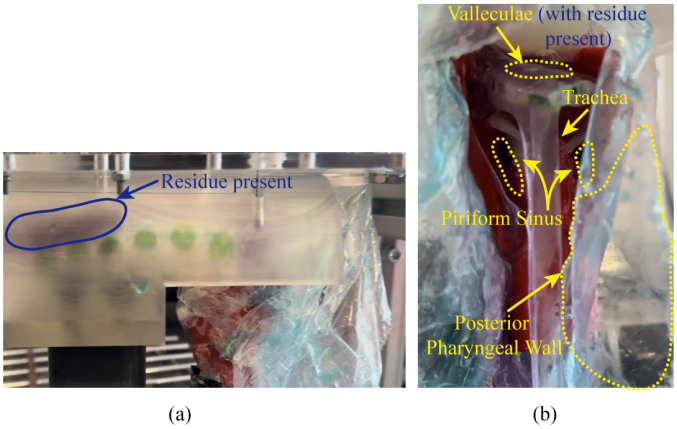


Fig. 12. Residue after multiple swallowing trials. (a) Residue in the oral cavity. (b) Residue in the pharynx (the oral-pharyngeal duct was cut open for better observation).

### *B. Swallowing Experiment (With food)*

*1) Experiment Setup:* To assess the swallowing capability and safety of the prototype and adhere to the International Dysphagia Diet Standardization Initiative (IDDSI) framework [46] for food textures and drink thickness, we prepared fluids of IDDSI Levels 1, 2, and 3, using guar gum as thickener, and measured following the IDDSI guidelines [47]. Before formal swallowing experiments, preliminary trials were conducted to determine the most suitable viscosity. During these trials, fluids of level 1 and 2 tended to leak anteriorly from the oral end of the duct before the actuation sequence was complete, reflecting an edge case. Therefore, level 3 fluids (moderately thick, with a thickness similar to that of runny pureed fruit), which demonstrated the most stable swallowing performance, were selected for the formal experiments. The tested material was dyed purple for enhanced visibility, and injected into the oral-pharyngeal duct.

*2) Results:* The swallowing experiment is shown in Fig. 11. The prototype successfully transports the fluid into the oropharynx. Fig. 12 shows the residue after one swallowing cycle. In the anterior region of the oral cavity (Fig. 12(a)), residue is observed. This occurs because the opening of the oropharyngeal duct is unsealed and extends beyond the tongue tip (Fig. 7(a)) for easier fluid injection. Consequently, when the tongue elevates, it inevitably pushes some fluid anterior and away from the tip of the tongue. The residue in the pharynx is shown in Fig. 12(b). Following the assessment method used in the swallowing simulator in [23], here, we assessed the swallowing safety using two qualitative clinical indicators, as also established in [48]: (a) the presence or absence of residue in the trachea, through visual observation; (b) a score from 1 to 6 based on the number of regions with detectable residue. A score of 1 is given when there is no residue. When residue is present, the scoring criteria are as follows: +1 point for residue in the valleculae, +2 points for residue in the piriform sinus, and +2 points for residue at the posterior pharyngeal wall. Consequently, the scores were assigned as shown in Table II. A higher score indicates lower swallowing safety and higher risk of aspiration.

After multiple swallowing trials with the tested fluid, as shown in Fig. 12(b), no residue was found in the trachea, indicating that the proposed model successfully prevented aspiration while swallowing. Furthermore, no residue was found in the piriform sinus and the posterior pharyngeal wall (represented by the surface of the cut-open oral-pharyngeal duct). Since the pharyngeal constrictor muscles were not

**IEEE Robotics and Automation Letters (RA-L) paper, presented at ICRA 2026, Vienna, Austria. Cite as RA-L paper.**

TABLE II
ASSESSMENT SCHEME OF SWALLOWING SAFETY

| Presence of Residue | Score |
|---|---|
| No residue | 1 |
| Valleculae Only | 2 |
| Posterior pharyngeal wall or piriform sinus only | 3 |
| Valleculae and posterior pharyngeal wall or piriform sinus | 4 |
| Posterior pharyngeal wall and piriform sinus | 5 |
| All three regions | 6 |

replicated in this work, the posterior pharyngeal wall did not contact the fluid, which differs from the physiological situation in real swallowing. Therefore, we conservatively assigned a score of 4, indicating a middle level of swallowing safety.

## IV. CONCLUSION

This paper presented a novel robotic model that emulates the oral and pharyngeal stages of human swallowing, with core design feature being a passive actuation system of the protective closure of the epiglottis. It contributes to addressing the physiological fidelity of epiglottis actuation within the field of swallowing robotics. The results indicate that the developed model can replicate the vertical motion of the tongue and the passive protective closure of the epiglottis during swallowing, proving qualitatively that the robot is capable of swallowing and that the epiglottis fulfills the requirement of preventing fluids from entering the trachea. The fluid can be successfully transported to the oropharyngeal cavity and, subsequently, descends through the pharynx under gravity, although some residue remains. Finally, a swallowing safety score of 4 was assigned, which is higher than that previously mentioned in the literature [23]. However, this work focuses on epiglottal actuation and does not replicate the pharyngeal constrictors.

Future work will focus on three main directions. First, sensor systems similar to that proposed in [49] could be integrated on the palate as well as in the oropharynx. The former can be used to measure the pressure between the tongue and the palate during swallowing. By comparing these measurements with physiological tongue-pressure data, the tongue actuation system can be further optimized to more closely replicate the detailed motion of the human tongue. The latter can detect the pressure exerted by the bolus on the pharyngeal wall during the oropharyngeal stage of swallowing, which can be used to trigger the involuntary pharyngeal stage of swallowing [50]. Such integration could enable more sophisticated control strategies including feedback-driven actuation and data-driven, machine learning-based modulation of swallowing dynamics. Second, the pharyngeal structures will be refined, particularly, by implementing partially overlapping, tendon-driven pharyngeal constrictor muscles in the oropharynx to replicate the involuntary and peristaltic contractions of the pharynx. Lastly, by adjusting parameters such as the velocity and range of laryngeal elevation [28], [51], edge cases of pathological swallowing patterns such as abnormal epiglottic motions can be simulated without introducing an arbitrary trajectory or a dedicated actuator. The ultimate goal is to replicate both the oral and pharyngeal stages of swallowing with fidelity to both swallowing anatomy and physiology, providing a reliable platform for dysphagia research and a safer, more ethical alternative for developing VMB.

## REFERENCES


[1] M. Koichiro and J. Palmer, "Anatomy and physiology of feeding and swallowing: Normal and abnormal," *Physical Medicine and Rehabilitation Clinics of North America*, vol. 19, no. 4, pp. 691–707, 2008.

[2] K. Yamamura *et al.*, "Neural mechanisms of swallowing and effects of taste and other stimuli on swallow initiation," *Biological and Pharmaceutical Bulletin*, vol. 33, no. 11, pp. 1786–1790, 2010.

[3] M. Su *et al.*, "Clinical applications of iddsi framework for texture recommendation for dysphagia patients," *Journal of Texture Studies*, vol. 49, no. 1, pp. 2–10, 2017.

[4] P. Clavé and R. Shaker, "Dysphagia: current reality and scope of the problem," *Nat Rev Gastroenterol Hepatol*, vol. 12, pp. 259–270, 2015.

[5] J. A. Cichero and K. W. Altman, "Definition, prevalence and burden of oropharyngeal dysphagia: a serious problem among older adults worldwide and the impact on prognosis and hospital resources," *Nestle Nutr Inst Workshop Ser*, vol. 72, pp. 1–11, 2012.

[6] E. Hurtte, J. Young, and C. P. Gyawali, "Dysphagia," *Primary Care: Clinics in Office Practice*, vol. 50, no. 3, pp. 325–338, 2023.

[7] R. L. Drake, A. W. Vogl, A. W. M. Mitchell, R. Tibbitts, and P. Richardson, *Gray's Atlas of Anatomy*, 2nd ed. Churchill Livingstone, 2014.

[8] B. Kertscher, R. Speyer, E. Fong, A. M. Georgiou, and M. Smith, "Prevalence of oropharyngeal dysphagia in the netherlands: a telephone survey," *Dysphagia*, vol. 30, pp. 114–120, 2015.

[9] C. Takizawa, E. Gemmell, J. Kenworthy, and R. Speyer, "A systematic review of the prevalence of oropharyngeal dysphagia in stroke, parkinson's disease, alzheimer's disease, head injury, and pneumonia," *Dysphagia*, vol. 31, pp. 434–441, 2016.

[10] M. Miarons Font and S. L. Rofes, "Antipsychotic medication and oropharyngeal dysphagia: systematic review," *Eur J Gastroenterol Hepatol*, vol. 29, no. 12, pp. 1332–1339, 2017.

[11] I. J. Cook *et al.*, "Aga technical review on management of oropharyngeal dysphagia," *Gastroenterology*, vol. 116, no. 2, pp. 455–478, 1999.

[12] O. Ortega, A. Martín, and P. Clavé, "Diagnosis and management of oropharyngeal dysphagia among older persons, state of the art," *Journ. of the American Medical Directors Association.*, vol. 18, no. 7, pp. 576–582, 2017.

[13] S. T. Coster and W. H. Schwarz, "Rheology and the swallow-safe bolus," *Dysphagia*, vol. 1, pp. 113–118, 1987.

[14] R. Shaker, C. Easterling, P. Belafsky, and G. Postma, *Manual of Diagnostic and Therapeutic Techniques for Disorders of Deglutition*. Springer, 2013.

[15] M. D. Ballesteros-Pomar, A. Cherubini, H. Keller, P. Lam, Y. Rolland, and S. F. Simmons, "Texture-modified diet for improving the management of oropharyngeal dysphagia in nursing home residents: An expert review," *The Journal of Nutrition, Health and Aging*, vol. 24, no. 6, pp. 576–581, 2020.

[16] E. Flynn, C. H. Smith, C. D. Walsh, and M. Walshe, "Modifying the consistency of food and fluids for swallowing difficulties in dementia," *Cochrane Database of Systematic Reviews*, no. 9, 2018.

[17] U. T. Andersen, A. M. Beck, A. Kjaersgaard, T. Hansen, and I. Poulsen, "Systematic review and evidence based recommendations on texture modified foods and thickened fluids for adults ($\geq$18 years) with oropharyngeal dysphagia," *e-SPEN Journal*, vol. 8, no. 4, pp. e127–e134, 2013.

[18] J. S. Shim, B. M. Oh, and T. R. Han, "Factors associated with compliance with viscosity-modified diet among dysphagic patients," *Annals of Rehabilitation Medicine*, vol. 37, no. 5, pp. 628–632, 2013.

[19] R. Newman, N. Vilardell, P. Clavé, and R. Speyer, "Effect of bolus viscosity on the safety and efficacy of swallowing and the kinematics of the swallow response in patients with oropharyngeal dysphagia: White paper by the european society for swallowing disorders (essd)," *Dysphagia*, vol. 31, p. 719, 2016.

[20] F. J. Chen, S. Dirven, W. L. Xu, J. Bronlund, X. N. Li, and A. Pullan, "Review of the swallowing system and process for a biologically mimicking swallowing robot," *Mechatronics*, vol. 22, no. 5, pp. 556–567, 2012.

[21] Y. Noh *et al.*, "Development of a robot which can simulate swallowing of food boluses with various properties for the study of rehabilitation of swallowing disorders," in *2011 IEEE International Conference on Robotics and Automation*, Shanghai, China, 2011, pp. 4676–4681.

**IEEE Robotics and Automation Letters (RA-L) paper, presented at ICRA 2026, Vienna, Austria. Cite as RA-L paper.**


[22] M. R. Mackley, C. Tock, R. Anthony, S. A. Butler, G. Chapman, and D. C. Vadillo, "The rheology and processing behavior of starch and gum-based dysphagia thickeners," *Journal of Rheology*, vol. 57, no. 6, pp. 1533–1553, 2013.

[23] Y. Fujiso, N. Perrin, J. van der Giessen, N. E. Vrana, F. Neveu *et al.*, "Swall-e: A robotic in-vitro simulation of human swallowing," *PLOS ONE*, vol. 13, no. 12, p. e0208193, 2018.

[24] M. Stading, M. Q. Waqas, F. Holmberg *et al.*, "A device that models human swallowing," *Dysphagia*, vol. 34, pp. 615–626, 2019.

[25] H. Sato, H. Kobayashi, K. Matsumoto, T. Hashimoto, and Y. Michiwaki, "Development of human-size swallowing robot," *Journal of Robotics and Mechatronics*, vol. 35, no. 6, pp. 1663–1674, 2023.

[26] J. Ziadeh, K. Junge, and J. Hughes, "Bio-inspired robotic swallowing simulator," in *2024 IEEE 7th International Conference on Soft Robotics*, San Diego, CA, USA, 2024, pp. 319–324.

[27] G. M. Ardran and F. H. Kemp, "The protection of the laryngeal airway during swallowing," *British Journal of Radiology*, vol. 25, no. 296, pp. 406–416, 2014.

[28] W. G. J. Pearson, B. K. Taylor, J. Blair, and B. Martin-Harris, "Computational analysis of swallowing mechanics underlying impaired epiglottic inversion," *Laryngoscope*, vol. 126, no. 8, pp. 1854–1858, 2016.

[29] J. A. Logemann, P. J. Kahrilas, J. Cheng, B. R. Pauloski, P. J. Gibbons, A. W. Rademaker, and S. Lin, "Closure mechanisms of laryngeal vestibule during swallow," *American Journal of Physiology-Gastrointestinal and Liver Physiology*, vol. 262, no. 2, pp. G338–G344, 1992.

[30] T. B. Talbot, "Balancing physiology, anatomy and immersion: How much biological fidelity is necessary in a medical simulation?" *Military Medicine*, vol. 178, no. suppl_10, pp. 28–36, 2013.

[31] S. Maglio, C. Park, S. Tognarelli, A. Menciassi, and E. T. Roche, "High-fidelity physical organ simulators: From artificial to bio-hybrid solutions," *IEEE Transactions on Medical Robotics and Bionics*, vol. 3, no. 2, pp. 349–361, 2021.

[32] G. M. Ardran and F. H. Kemp, "The mechanism of the larynx—ii the epiglottis and closure of the larynx," *British Journal of Radiology*, vol. 40, no. 473, pp. 372–389, 2014.

[33] M. W. Donner, J. F. Bosma, and D. L. Robertson, "Anatomy and physiology of the pharynx," *Gastrointestinal Radiology*, vol. 10, no. 3, pp. 196–212, 1985.

[34] O. Ekberg and S. V. Sigurjónsson, "Movement of the epiglottis during deglutition," *Gastrointest Radiol*, vol. 7, pp. 101–107, 1982.

[35] R. Interactive. (2023) Gameready human mouth and tongue. Accessed: Apr. 17, 2025. [Online]. Available: https://sketchfab.com/3d-models/gameready-human-mouth-and-tongue-6c25fc725d1c404c82ec7499e4f7e041

[36] U. of Dundee School of Medicine. (2020) Anatomy of the larynx. Accessed: Apr. 17, 2025. [Online]. Available: https://sketchfab.com/3d-models/anatomy-of-the-larynx-a00bc73a303c46248db6a13a88b23404

[37] F. Faure, C. Duriez, H. Delingette, J. Allard, B. Gilles, S. Marchesseau, H. Talbot, H. Courtecuisse, G. Bousquet, I. Peterlik, and S. Cotin, *SOFA: A Multi-Model Framework for Interactive Physical Simulation*. Berlin, Heidelberg: Springer Berlin Heidelberg, 2012, pp. 283–321.

[38] Inria, USTL, UJF, CNRS, and MGH. (2025) Bilaterallagrangianconstraint. SOFA Framework Documentation. Accessed: Apr. 17, 2025. [Online]. Available: https://sofa-framework.github.io/doc/components/constraint/lagrangian/model/bilaterallagrangianconstraint/

[39] Inria, USTL, UJF, CNRS, and MGH. (2025) Fixedprojectiveconstraint. SOFA Framework Documentation. Accessed: Apr. 17, 2025. [Online]. Available: https://sofa-framework.github.io/doc/components/constraint/projective/fixedprojectiveconstraint/

[40] A. Shibata, M. Higashimori, I. G. Ramirez-Alpizar, and M. Kaneko, "Tongue elasticity sensing with muscle contraction monitoring," in *2012 ICME International Conference on Complex Medical Engineering (CME)*, Kobe, Japan, 2012, pp. 511–516.

[41] Y. Liu, Y. Chen, W. Yim, and R. C. Wang, "Study of the suture-patch device through the tongue for sleep apnea using fluid-structure interaction modeling," *Journal of Otolaryngology and Rhinology*, vol. 4, p. 048, 2018.

[42] C. M. Pauken, R. Heyes, and D. G. Lott, "Mechanical, cellular, and proteomic properties of laryngotracheal cartilage," *Cartilage*, vol. 10, no. 3, pp. 321–328, 2019.

[43] J. Vaicekauskaite, P. Mazurek, S. Vudayagiri, and A. L. Skov, "Mapping the mechanical and electrical properties of commercial silicone elastomer formulations for stretchable transducers," *Journal of Materials Chemistry C*, vol. 8, no. 4, pp. 1273–1279, 2020.

[44] A. Oh, D. Park, K.-S. Han, and T. Oh, "Elastic modulus of locally stiffness-variant polydimethylsiloxane substrates for stretchable electronic packaging applications," *Journal of the Microelectronics and Packaging Society*, vol. 22, pp. 91–98, 2015.

[45] NeuRA - Neuroscience Research Australia. (2021) How cool is this? new real-time mri technique captures the complex dynamics of swallowing. Facebook. Accessed: Apr. 17, 2025. [Online]. Available: https://www.facebook.com/watch/?v=188254676551363

[46] J. A. Y. Cichero, P. Lam, C. M. Steele, B. Hanson, J. Chen, R. O. Dantas, J. Duivestein, J. Kayashita, C. Lecko, J. Murray, M. Pillay, L. Riquelme, and S. Stanschus, "Development of international terminology and definitions for texture-modified foods and thickened fluids used in dysphagia management: The iddsi framework," *Dysphagia*, vol. 32, pp. 293–314, 2017.

[47] International Dysphagia Diet Standardisation Initiative. (2019) Complete iddsi framework detailed definitions 2.0. IDDSI Framework Documents. Accessed: Apr. 28, 2025. [Online]. Available: https://www.iddsi.org/images/Publications-Resources/DetailedDefnTestMethods/English/V2DetailedDefnEnglish31july2019.pdf

[48] T. I. Omari, E. Dejaeger, D. Van Beckevoort, A. Goeleven, P. De Cock, I. Hoffman, M. H. Smet, G. P. Davidson, J. Tack, and N. Rommel, "A novel method for the nonradiological assessment of ineffective swallowing," *The American Journal of Gastroenterology*, vol. 106, no. 10, pp. 1796–1802, 2011.

[49] K. Hori, T. Ono, K.-i. Tamine, J. Kondo, S. Hamanaka, Y. Maeda, J. Dong, and M. Hatsuda, "Newly developed sensor sheet for measuring tongue pressure during swallowing," *Journal of Prosthodontic Research*, vol. 53, no. 1, pp. 28–32, 2009.

[50] P. Hall, John E. and M. M. Hall, Michael E., "Propulsion and mixing of food in the alimentary tract," in *Guyton and Hall Textbook of Medical Physiology (Fourteenth Edition)*, P. Hall, John E. and M. M. Hall, Michael E., Eds. Elsevier, 2021, pp. 797–806.

[51] J. Zhang, Y. Zhou, N. Wei, B. Yang, A. Wang, H. Zhou, X. Zhao, Y. Wang, L. Liu, M. Ouyoung, B. Villegas, and M. Groher, "Laryngeal elevation velocity and aspiration in acute ischemic stroke patients," *PLOS ONE*, vol. 11, no. 9, pp. 1–13, 2016.